DOI: 10.1002/ejic.200600070

Synthesis, Structure and Magnetic Properties of a New Low-Spin Iron(III) Complex [FeL_3] {L = [$HNC(CH_3)]_2C(CN)$}

Junichi Nishijo[a] and Nobuyuki Nishi*[a]

Keywords: Iron / Magnetic properties / N ligands

High-temperature treatment of acetonitrile with CaC_2 and $FeCl_2$ afforded crystals of the new iron(III) $S = 1/2$ low-spin complexes [FeL_3]ROH (R = CH_3 or C_2H_5), whose crystal structures were determined by single-crystal X-ray structural analysis. The methanol complex consists of a one-dimensional arrangement of the iron moieties, while each methanol molecule is separated from each other by the complexes. On the other hand, the ethanol complex contains a two dimensional arrangement of the iron moieties and one dimensionally aligned ethanol molecules elongated perpendicular to the sheet. Because of the large difference in the inter-complex overlap patterns between the ligands, the two materials show quite different magnetic properties. The magnetism of the crystal containing ethanol is well described by the singlet–triplet model with the antiferromagnetic interaction $2J/k_B = -7.5$ K, while that containing methanol obeys the Curie law with a negligibly small Weiss temperature.

Introduction

Transition-metal complexes of π-conjugated N-ligands have attracted much attention over the years. In these complexes, the strong coordination bonds with the lone pair of the nitrogen atoms bring the d-electrons of the transition metal and the π-electrons of the ligands close to each other, and the interaction between d- and π-electrons leads to several important properties, such as a modified reactivity of the center metal, high photon absorbance and efficient charge transfer. Previous studies with such complexes have revealed their usefulness as catalysts[1–7] and dye-sensitized solar cells.[8–10] From the viewpoint of molecule-based magnets, this kind of complex would offer a strong spin–spin interaction as the strong metal–nitrogen interaction brings about a high spin density at the nitrogen atom. On the other hand, it is known that the π-electrons can convey spin polarization from one side of the molecule to the other side through the π-conjugated system.[11–13] Because a π-conjugated N-ligand has both of these features, it is expected that transition-metal complexes based on these ligands would enable a strong, long-range spin–spin interaction.[14–18] Furthermore, the flat π-conjugated molecules tend to stack their molecular planes, which results in a large intermolecular orbital overlap and thus a strong intermolecular spin–spin interaction.[19,20]

The strong coordination bond is also essential to investigate the effect of the intermolecular arrangement on the magnetism. It is well known that the magnetism of molecule-based magnets largely depends on the intermolecular overlap patterns, and that some of them can be controlled by the absorption/desorption of solvent.[21–23] By using π-conjugated N ligands, the complex approximately keep its intra-complex structure thanks to the rigidness of the ligand and the strong coordination bonds, while the inter-complex arrangement is considerably rearranged upon changing the solvent molecules;[24,25] that is, we can investigate only the effect of the inter-complex arrangement.

Because of the features mentioned above, it is important to synthesize new transition-metal complexes of π-conjugated N-ligands. We decided to use the bidentate ligand 2-amino-3-cyanopent-2-en-4-imine (HL, Figure 1) for the following two reasons. First, its bidentate nature is promising to create magnetic complexes because they are likely to form stable coordination bonds like bipyridine. Secondly, the planer shape of the ligand and the protruding cyano group seem to ease the intermolecular orbital overlaps which causes inter-complex spin–spin interaction. However, although the structure of this ligand is attractive, its instability prevents the easy synthesis of complexes. Thus, although it was first synthesized more than 40 years ago,[26,27]

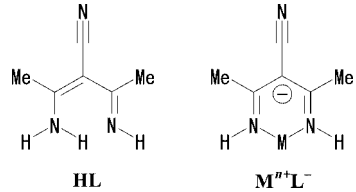

Figure 1. The molecular structure of 2-amino-3-cyanopent-2-en-4-imine (HL). The deprotonated form of the molecule behaves as a bidentate ligand ($M^{n+}L^-$).

[a] Institute for Molecular Science,
Nishigo-naka 38, Myodaiji, Okazaki 444-8585, Japan
E-mail: nishi@ims.ac.jp

up to the present time only one complex of Co and a few complexes of Ga, Al, and In with the deprotonated ligand (L^-) have been synthesized.[28–30] In this paper, we report new transition-metal complexes based on this ligand synthesized by an unconventional method, and report the remarkable solvent dependency of their structure and magnetism.

Results and Discussion

Synthesis

To obtain the transition-metal complex based on the ligand, we tried to develop a new synthesis method by using a strong base under water-free conditions. It is known that the ligand can be synthesized by the trimerization of acetonitrile molecules in the presence of a strong base, as shown in Scheme 1.[28–30] Furthermore, the strong base stabilizes the deprotonated form of the ligand and enables complex formation. Because the ligand is easily decomposed in the presence of water molecules,[27] the synthesis should be done under strictly water-free conditions. In light of these two conditions, calcium carbide is one of the most suitable reagents as a strong base because it is an easily acquired water-free base that is strong enough to deprotonate acetonitrile molecules. A stainless-steel airtight vessel is appropriate for the synthesis as this not only allows exclusion of water from the air but also enables the synthesis to be performed at high temperature, where the trimerization of acetonitrile is accelerated. Despite the water-sensitivity of the free ligand molecule, the complex [FeL_3] is stable even in air. It should be noted that vigorous stirring, a longer reaction time, or a higher reaction temperature lead only to carbon-encapsulated iron nanoparticles due to the reductive nature of C_2^{2-}.[31] This one-pot synthesis method gives the complex [FeL_3].

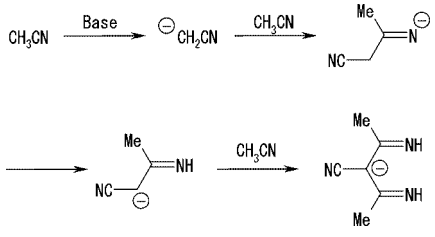

Scheme 1.

Crystal Structures

The complex was obtained as a racemic crystal regardless of the solvent molecules. The unit cells of [FeL_3]CH_3OH and [FeL_3]C_2H_5OH contain two crystallographically equivalent Δ- and Λ-[FeL_3] and one Δ- and one Λ-[FeL_3] moieties, respectively. Selected bond lengths and angles, and the molecular structures of [FeL_3]ROH can be found in Tables 1 and 2, and Figures 2 and 3, respectively. The intra-complex structures are nearly identical regardless of the solvent molecules. Each complex consists of an iron atom and three chelating ligand molecules such that the iron atom is surrounded by the six nitrogen atoms of the ligands to form an octahedral FeN_6 chromophore. The six Fe–N bonds have similar lengths, and no Jahn–Teller distortion was observed at room temperature despite the low-spin d^5 configuration of iron(III), as evidenced by the small Curie constant (discussed later). The Fe–N bond lengths of [FeL_3]ROH range from 1.916(4) to 1.957(3) Å and are in reasonable agreement with the values for other iron complexes with Schiff-base-type ligands.[32,33] The intra-ligand bond lengths are close to those of other complexes of the L^- ligand reported previously.[28–30] The C–N bond lengths, which range from 1.292(6) to 1.316(5) Å, and the π-conjugated C–C bond lengths, which range from 1.406(7) to 1.433(6) Å, indicate that the negative charges are delocalized over the π-conjugated system of the ligand. Because of this aromaticity, the six-membered chelate rings tend to be planar except for a small inflection at the coordinated nitrogen atoms. For example, the torsion angles of Fe1–N1–N2–C3, Fe1–N4–N5–C9, and Fe1–N8–N7–C15 in the [FeL_3]CH_3OH crystal have values [172.74(13)°, 155.84(13)°, and 166.69(13)°, respectively] that are slightly smaller than 180°, while the ligand molecules keep its almost flat structure.

Table 1. Selected bond lengths [pm] and angles [°] for [FeL_3]-CH_3OH.

Fe1–N1	192.3(3)	N8–C16	130.5(4)
Fe1–N2	192.4(3)	C2–C3	142.4(4)
Fe1–N4	192.6(3)	C3–C4	142.4(5)
Fe1–N5	193.8(3)	C3–C6	141.7(5)
Fe1–N7	195.7(3)	C8–C9	142.1(4)
Fe1–N8	193.0(3)	C9–C10	142.5(4)
N1–C2	130.0(4)	C9–C12	141.6(4)
N2–C4	130.1(4)	C14–C15	142.2(5)
N4–C8	130.5(4)	C15–C16	142.1(5)
N5–C10	130.6(4)	C15–C18	142.7(5)
N7–C14	129.8(4)		
N1–Fe1–N7	177.82(11)	N1–Fe1–N2	90.80(12)
N2–Fe1–N5	178.81(12)	N4–Fe1–N5	88.17(12)
N4–Fe1–N8	177.67(12)	N7–Fe1–N8	87.96(13)

Table 2. Selected bond lengths [pm] and angles [°] for [FeL_3]-C_2H_5OH.

Fe1–N1	192.6(4)	N8–C15	131.4(6)
Fe1–N2	191.6(4)	C1–C2	142.4(6)
Fe1–N4	193.2(4)	C2–C3	142.8(6)
Fe1–N5	195.4(4)	C2–C6	142.4(6)
Fe1–N7	195.3(4)	C7–C8	142.2(6)
Fe1–N8	195.3(4)	C8–C9	141.8(7)
N1–C1	129.6(6)	C8–C12	142.3(6)
N2–C3	130.8(6)	C13–C14	143.5(7)
N4–C7	131.6(5)	C14–C15	140.6(7)
N5–C9	130.5(6)	C14–C18	143.3(6)
N7–C13	129.2(6)		
N1–Fe1–N5	177.57(16)	N1–Fe1–N2	90.39(16)
N2–Fe1–N7	176.22(16)	N4–Fe1–N5	88.43(17)
N4–Fe1–N8	176.83(16)	N7–Fe1–N8	87.05(17)

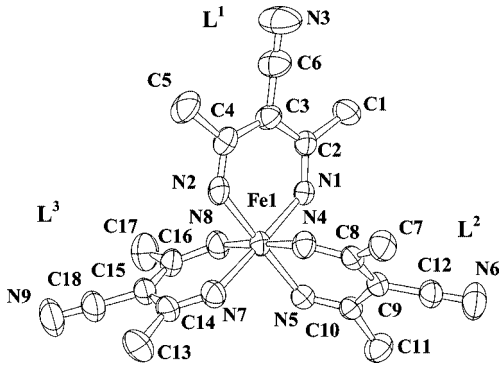

Figure 2. Thermal ellipsoid plot (50% probability) of $[FeL_3]$-CH_3OH. The labels L^i identify the three crystallographically independent ligand molecules. A methanol molecule and hydrogen atoms have been omitted for clarity.

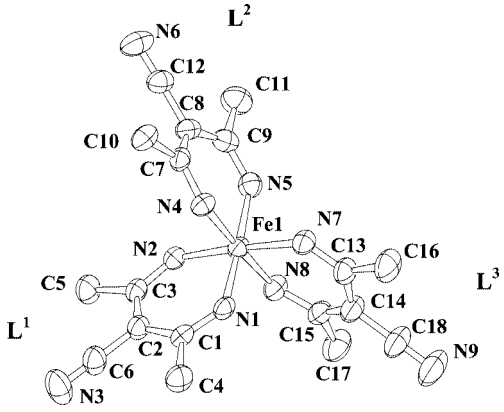

Figure 3. Thermal ellipsoid plot (50% probability) of $[FeL_3]$-C_2H_5OH. The labels L^i identify the three ligand molecules. An ethanol molecule and hydrogen atoms have been omitted for clarity.

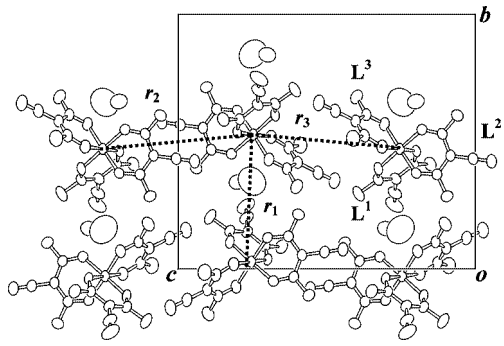

Figure 4. The crystal structure of $[FeL_3]CH_3OH$ viewed along the *a* axis. Hydrogen atoms have been omitted for clarity. The dotted lines indicate the short iron–iron distances (see text).

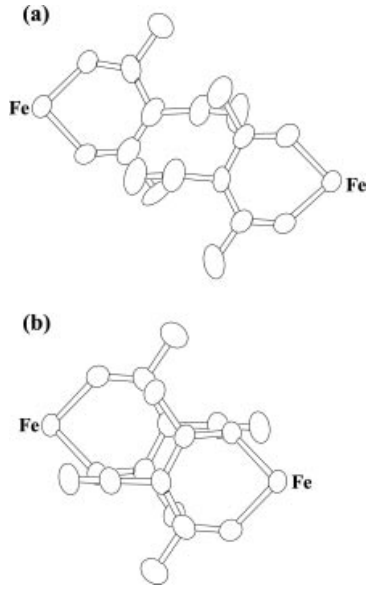

Figure 5. The two kinds of stacking modes between adjacent ligands viewed perpendicular to the six-membered chelate rings: a) Type A, b) Type B (see text). Hydrogen atoms have been omitted for clarify.

In contrast to the intra-complex structure, the inter-complex arrangement depends greatly on the solvent. In the crystal of $[FeL_3]CH_3OH$, each $[FeL_3]$ moiety has two short contacts with two adjacent complexes, as shown in Figure 4, and the ligands L^2 and L^3 face their counterparts in adjacent complexes. The complexes are connected to each other by these short ligand–ligand contacts and are arranged one-dimensionally parallel to the *c* axis. The cyano group of ligand L^1 is directed towards the hydroxy group of a neighboring methanol molecule. The stacking structures of L^2–L^2 and L^3–L^3 resemble each other. This stacking mode (type A) is shown in Figure 5 (a), where the cyano groups of the ligands are placed at the midpoints of the C–C bonds between the imine groups and methyl groups. In these contacts, the interatomic distance between the nitrogen atom of the cyano group and the carbon atom of the imine group is about 3.5 Å. In type-A stacking, the overlap between π-orbitals of the ligands is expected to be small due to the displacement of the two six-membered chelate rings, thus suggesting a weak spin–spin interaction between the complexes. The short iron–iron distances in the *bc* plane (Figure 4) are r_1 = 8.495(5), r_2 = 9.359(5), and r_3 = 9.337(5) Å, while that in the *a* direction is 8.099(5) Å.

The crystal structure of $[FeL_3]C_2H_5OH$ is characterized by a two-dimensional cage-like arrangement of the complexes and one-dimensionally aligned ethanol molecules. In the crystal, four complexes form a cage that encloses an ethanol molecule, as shown in Figure 6, and this cage-like structure spreads as a sheet in the *bc* plane. Each ligand in a sheet is close to a neighboring crystallographically equivalent ligand, and the stacking mode of the ligand pairs L^1–L^1 and L^3–L^3 is also classified as type A (see Figure 5), with an N–C interatomic contact of about 3.5 Å, while that of L^2–L^2 is of type B, with an interatomic distance of around 3.8 Å between the carbon atom of the cyano group and the carbon or nitrogen atom of the imine group. Although the interatomic distance of type B stacking is longer than that of type A, it is expected that the larger π-orbital overlap of type B stacking brings about a stronger spin–spin interaction than that of type A. The sheets of the cage-like structures are stacked along the *a* axis, where the adjacent sheets are weakly bonded by the inter-plane type A stacking of L^2

ligands. In short, one complex has two small intra-sheet overlaps (type A, L^1–L^1 and L^3–L^3), one small inter-sheet overlap (type A, L^2–L^2), and one large intra-sheet overlap (type B, L^2–L^2). The cavities of the cages are connected and form one-dimensional tunnel structures that are elongated parallel to the *a* axis; these are filled with ethanol molecules. The short iron–iron distances in the *bc* plane shown in Figure 6 are r_1 = 8.142(4), r_2 = 10.881(4), and r_3 = 9.337(4) Å, while that in the *a* direction is 8.195(3) Å. The shortest iron–iron distance in the crystal of $[FeL_3]C_2H_5OH$ is therefore slightly longer than that of $[FeL_3]CH_3OH$.

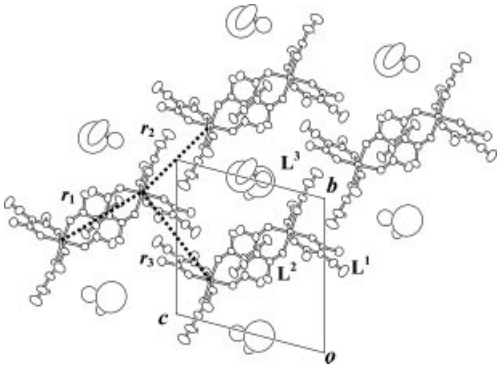

Figure 6. The crystal structure of $[FeL_3]C_2H_5OH$ viewed along the *a* axis. Hydrogen atoms have been omitted for clarify. The dotted lines indicate the short iron–iron distances (see text).

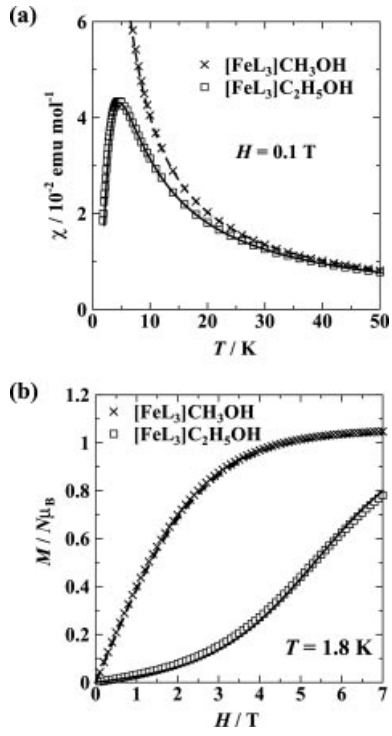

Figure 7. a) The magnetic susceptibilities and b) the reduced magnetization curves of $[FeL_3]ROH$. The dashed lines are the theoretical curves for the free S = 1/2 spins having g = 2.08, and the solid lines are the theoretical curves based on the singlet–triplet model with the values of $2J/k_B$ = –7.5 K and g = 2.08 (see text).

Magnetic Properties

The temperature dependencies of the magnetic susceptibilities, χ, of $[FeL_3]ROH$ and the magnetization curves at 1.8 K are shown in Figure 7 (parts a and b), respectively. The magnetic susceptibility of $[FeL_3]CH_3OH$ follows the Curie–Weiss law in the whole temperature range, with a Curie constant, C, of 0.406 emu K mol^{-1} and a negligibly small Weiss temperature, Θ. The fact that Θ is almost zero indicates that the type A overlap of the ligands does not contribute to the spin–spin interaction due to the poor overlap of the π-orbitals. The observed value of C roughly agrees with the spin-only value for a S = 1/2 species (0.375), thereby indicating the low-spin nature of the iron(III). The small enhancement of C from that of a free S = 1/2 spin can be attributed to the slightly larger g value predicted from the magnetization curve. The magnetization curve of $[FeL_3]CH_3OH$ is very close to the Brillouin curve of S = 1/2 spins with a g value of 2.08, which indicates that the inter-complex spin–spin interaction is negligible.

The magnetic susceptibility of $[FeL_3]C_2H_5OH$ can also be described by the Curie–Weiss law in the high-temperature region above 10 K (C = 0.403 emu K mol^{-1}, Θ = –3.3 K). Below 10 K, χ reaches a peak at 4.6 K and then decreases rapidly with decreasing temperature. A linear extrapolation of χ to lower temperature gives χ = 0 at a finite temperature of 0.7 K, thus suggesting that the ground state of the spin system is a singlet. Despite the longer iron–iron distance and smaller spin density of $[FeL_3]C_2H_5OH$ relative to those of $[FeL_3]CH_3OH$, the inter-complex spin–spin interaction of $[FeL_3]C_2H_5OH$ is stronger than that of $[FeL_3]$-CH_3OH. This fact confirms that the spin–spin interaction is strongly dependent on the inter-ligand overlap of the π-orbitals, as predicted from the crystal structures, as in some previously reported materials, where ligand–ligand contacts play important roles.[34,35] Based on the crystal structure, where only one strong inter-complex interaction is expected, a singlet–triplet model is the appropriate for the spin system of $[FeL_3]C_2H_5OH$. In this model, the spin Hamiltonian, H, is described as shown in Equation (1), where J, S_i, g, μ_B, and H_{ex} are the interaction between spins, the spin values, the g value, the Bohr magneton, and the external magnetic field, respectively.

$$H = -2JS_1 \cdot S_2 + g\mu_B \sum_i S_i \cdot H_{ex} \quad (1)$$

By using this spin Hamiltonian, the partition function Z [Equation (2)], the free energy F [Equation (3)], the magnetization, M, and χ can be calculated, as shown in Equations (4) and (5), where N and k_B are the Avogadro number and the Boltzmann constant, respectively. The best fit, shown as solid lines in parts a and b of Figures 7 is nearly indistinguishable from the observed values with the adjustable parameters of $2J/k_B$ = –7.5 K and g = 2.08. This consistency offers evidence that only the type B overlap can bring about a strong spin–spin interaction.

$$Z = T_r \exp(-H/k_B T) \quad (2)$$

$$F = -k_B T \cdot \ln Z \quad (3)$$

$$M(H_{ex},T) = -\frac{\partial F}{\partial H_{ex}} = \frac{Ng\mu_B \exp(2J/k_B T)\sinh(g\mu_B H_{ex}/k_B T)}{1+\exp(2J/k_B T)[1+2\cosh(g\mu_B H_{ex}/k_B T)]} \quad (4)$$

$$\chi(T) = \left(\frac{\partial M}{\partial H_{ex}}\right)_{H_{ex}=0} = \frac{Ng^2\mu_B{}^2}{k_B T}\frac{1}{3+\exp(-2J/k_B T)} \quad (5)$$

Conclusions

Crystals of the new iron(III) complex $[FeL_3]$ containing ROH (R = CH_3 and C_2H_5) have been obtained. The crystal structure of $[FeL_3]CH_3OH$ is characterized by a one-dimensional arrangement of the $[FeL_3]$ moieties where the cyano groups are placed above the methyl groups of adjacent moieties. Because of the small overlap between the π-orbitals of the ligands, the inter-complex spin–spin interaction of $[FeL_3]CH_3OH$ is weak, as evidenced by the almost zero value of the Weiss temperature and the absence of a magnetic transition. On the other hand, the crystal of $[FeL_3]$-C_2H_5OH consists of a two-dimensional sheet-like arrangement of $[FeL_3]$ moieties and one-dimensionally aligned ethanol molecules elongated perpendicular to the sheets. In this structure, $[FeL_3]$ moieties are dimerized by the large inter-ligand overlap and a cyano group is placed above an imine group of the neighboring complex. Owing to the dimerization of the complexes, the magnetic properties of $[FeL_3]C_2H_5OH$ are consistent with a singlet–triplet model with the inter-complex spin–spin interaction $2J/k_B$ = –7.5 K.

Experimental Section

Materials and Measurements: CaC_2 (Kojundo Chemical Lab. Co.) was used after ball-milling under argon for 12 h, while $FeCl_2$ and anhydrous acetonitrile were used as supplied. IR spectra were recorded with a Shimadzu FTIR-8600PC for KBr disks. Elemental analysis was performed with a Yanaco MT-6. Single-crystal X-ray diffraction data were collected with a Rigaku AFC7R MERCURY CCD diffractometer with graphite-monochromated Mo-K_α radiation (λ = 0.71069 Å) and a rotating anode generator (50 kV, 100 mA). The structures were solved by direct methods (SHELXS-97), then refined with full-matrix least-squares (SHELXL-97).[36] Graphics were produced with ORTEP-III.[37] The positions of hydrogen atoms, except N-H groups, were refined with a "riding" model with U_{iso} = 1.2 U_{eq} of the connected non-hydrogen atom or as ideal CH_3 groups with U_{iso} = 1.5 U_{eq}. The crystal data of $[FeL_3]$-ROH are shown in Table 3.

Table 3. Crystallographic data for $[FeL_3]$ROH.

	$[FeL_3]CH_3OH$	$[FeL_3]C_2H_5OH$
Crystal system	monoclinic	triclinic
Space group	$P2_1/n$	$P\bar{1}$
a [Å]	8.099(5)	8.195(2)
b [Å]	15.576(5)	12.736(3)
c [Å]	18.563(5)	13.404(2)
α [°]	90	73.149(2)
β [°]	79.690(5)	68.550(2)
γ [°]	90	81.190(3)
V [Å^3]	2303.9(17)	1244.4(5)
Z	4	2
ρ	1.310	1.127
F(000)	956	442
Crystal size [mm]	0.53×0.44×0.38	0.08×0.07×0.05
Temperature [K]	296.15	296.16
Absorption correction	numerical	numerical
Index range (h,k,l)	$-9 \le h \le 10$	$-9 \le h \le 10$
	$-16 \le k \le 20$	$-15 \le k \le 16$
	$-23 \le l \le 21$	$-17 \le l \le 15$
No. of reflections	21966	6034
No. of unique reflections	5144	4384
No. of reflections [$F > 2\sigma(F)$]	4791	3820
Residuals [$I > 2\sigma(I)$]	R_1 = 0.0696	R_1 = 0.0715
	wR_2 = 0.1678	wR_2 = 0.2090
Residuals (all data)	R_1 = 0.0742	R_1 = 0.0823
	wR_2 = 0.1710	wR_2 = 0.2183

CCDC-295169 and -295168 contain the supplementary crystallographic data for this paper. These data can be obtained free of charge from The Cambridge Crystallographic Data Centre via www.ccdc.cam.ac.uk/data_request/cif.

A Quantum Design MPMS-XL SQUID magnetometer was used to measure DC magnetic susceptibilities of $[FeL_3]$ROH between 300 and 1.8 K in a 0.1-T static magnetic field. The core temperature independent diamagnetic susceptibility was subtracted from the experimental values based on Pascal's constants for all constituent atoms.

Reaction: In a water- and oxygen-free glove box, CaC_2 (449 mg, 7 mmol) and $FeCl_2$ (634 mg, 5 mmol) were suspended in anhydrous acetonitrile (300 mL). The suspension was sealed in a SUS-316 stainless-steel high-temperature, high-pressure reactor (TPR-1, Taiatsu techno, Tokyo, Japan), then the solution was heated to 240 °C at around 3 MPa for 12 h with gentle stirring. After cooling to room temperature, the solution was exposed to air and absolute methanol (100 mL) was added. Vigorous stirring of the solution for 20 min under air resulted in a deep-blue solution, which was then filtered. The residue was extracted with methanol, and the extract was added to the filtrate. The solution was dried in vacuo, then the precipitate was washed with toluene (200 mL) and extracted with dichloromethane (300 mL). The solution was dried in vacuo again. The blue powder was dissolved in hot methanol (20 mL), then cooled to –10 °C. The purple crystalline product was collected by filtration. Recrystallization from hot methanol gave 85 mg of $[FeL_3]CH_3OH$ (4%) as reddish-purple block crystals. $C_{19}H_{28}FeN_9O$ (454.34): calcd. C 50.23, H 6.21, N 27.75; found C 50.18, H 6.40 N 27.61. IR (KBr): ν(N–H) = 3280 cm^{-1}; ν_2(C≡N) = 2177; ν(C=N) = 1582 cm^{-1}. A single crystal of $[FeL_3]C_2H_5OH$ was obtained as follows. Pure $[FeL_3]CH_3OH$ crystals were dissolved in a mixture of THF (30 mL) and ethanol (10 mL). The solution was slowly evaporated at ambient pressure, and subsequent filtration gave small, deep-purple crystals. $C_{20}H_{30}FeN_9O$ (468.37): calcd. C 51.29, H 6.46, N 26.92; found C 51.23, H 6.25 N 26.99. IR (KBr): ν(N–H) = 3284 cm^{-1}; ν(C≡N) = 2182; ν(C=N) = 1579 cm^{-1}.

Acknowledgments

This work was supported by a program entitled "Research for the Future of Japan Society of the Promotion of Science" (RFTF: 99P01201). Part of this work was also supported by a Grant-in-Aid for Scientific Research (13NP0201) and the "Nanotechnology Support Project" of the Ministry of Education, Culture, Sports, Science and Technology (MEXT), Japan.

[1] D. E. De Vos, M. Dams, B. F. Sels, P. A. Jacobs, *Chem. Rev.* **2002**, *102*, 3615–3640 and references cited therein.
[2] R. Belzen, R. A. Klein, H. Kooijman, N. Veldman, A. L. Spek, C. J. Elsevier, *Organometallics* **1998**, *17*, 1812–1825.
[3] T. E. Patten, C. Troeltzsch, M. M. Olmstead, *Inorg. Chem.* **2005**, *44*, 9197–9206.
[4] T. Okada, N. Arimura, C. Ono, M. Yuasa, *Electrochim. Acta* **2005**, *51*, 1130–1139.
[5] S.-I. Murahashi, S. Noji, T. Hirabayashi, N. Komiya, *Tetrahedron: Asymmetry* **2005**, *16*, 3527–3535.
[6] I. Luobeznova, M. Raizman, I. Goldberg, Z. Gross, *Inorg. Chem.* **2006**, *45*, 386–394.
[7] Y. N. Belokon′, S. Caveda-Cepas, B. Green, N. S. Ikonnikov, V. N. Khrustalev, V. S. Larichev, M. A. Moscalenko, M. North, C. Orizu, V. I. Tararov, M. Tasinazzo, G. I. Timofeeva, L. V. Yashkina, *J. Am. Chem. Soc.* **1999**, *121*, 3968–3973.
[8] M. K. Nazeeruddin, A. Kay, I. Rodicio, R. Humphry-Baker, E. Müller, P. Liska, N. Vlachopoulos, M. Grätzel, *J. Am. Chem. Soc.* **1993**, *115*, 6382–6390.
[9] U. Bach, D. Lupo, P. Comte, J. E. Moser, F. Weissörtel, J. Salbeck, H. Spreitzer, M. Grätzel, *Nature* **1998**, *395*, 583–585.
[10] A. S. Polo, M. K. Itokazu, N. Y. M. Iha, *Coord. Chem. Rev.* **2004**, *248*, 1343–1361 and references cited therein.
[11] H. Iwamura, *Pure Appl. Chem.* **1993**, *65*, 57–64.
[12] H. Oshio, H. Ichida, *J. Phys. Chem.* **1995**, *99*, 3294–3302.
[13] I. Seggern, F. Tuczek, W. Bensch, *Inorg. Chem.* **1995**, *34*, 5530–5547.
[14] M. Ferbinteanu, H. Miyasaka, W. Wernsdorfer, K. Nakata, K. Sugiura, M. Yamashita, C. Coulon, R. Clérac, *J. Am. Chem. Soc.* **2005**, *127*, 3090–3099.
[15] J.-P. Costes, F. Dahan, A. Dupuis, *Inorg. Chem.* **2000**, *39*, 165–168.
[16] E. Colacio, M. Ghazi, R. Kivekäs, J. M. Moreno, *Inorg. Chem.* **2000**, *39*, 2882–2890.
[17] C.-M. Liu, S. Gao, D.-Q. Zhang, Y.-H. Huang, R.-G. Xiong, Z.-L. Liu, F.-C. Jiang, D.-B. Zhu, *Angew. Chem. Int. Ed.* **2004**, *43*, 990–994.
[18] H. Oshio, N. Hoshino, T. Ito, M. Nakano, *J. Am. Chem. Soc.* **2004**, *126*, 8805–8812.
[19] S. S. Turner, D. L. Pevelen, P. Day, K. Prout, *J. Chem. Soc., Dalton Trans.* **2000**, 2739–2744.
[20] S. S. Turner, C. Michaut, S. Durot, P. Day, T. Gelbrich, M. B. Hursthouse, *J. Chem. Soc., Dalton Trans.* **2000**, 905–909.
[21] W. Fujita, K. Awaga, *J. Am. Chem. Soc.* **1997**, *119*, 4563–4564.
[22] O. Kahn, J. Larionova, J. V. Yakuhmi, *Chem. Eur. J.* **1999**, *5*, 3443–3449.
[23] D. Maspoch, D. Ruiz-Molina, K. Wurst, N. Domingo, M. Cavallini, F. Biscarini, J. Tejada, C. Rovira, J. Veciana, *Nat. Mater.* **2003**, *2*, 190–195.
[24] M. Hostettler, K. W. Törnroos, D. Chernyshov, B. Vangdal, H.-B. Bürgi, *Angew. Chem. Int. Ed.* **2004**, *43*, 4589–4594.
[25] M. C. Giménez-López, M. Clemente-León, E. Coronado, F. M. Romero, S. Shova, J.-P. Tuchagues, *Eur. J. Inorg. Chem.* **2005**, 2783–2787.
[26] K. L. Wierzchiwski, D. Shugar, A. R. Kataritzky, *J. Am. Chem. Soc.* **1963**, *85*, 827–828.
[27] K. L. Wierzchiwski, D. Shugar, *Photochem. Photobiol.* **1963**, *2*, 377–391.
[28] M. R. Kopp, B. Neumüller, *Z. Anorg. Allg. Chem.* **1999**, *625*, 739–745; M. R. Kopp, B. Neumüller, *Z. Anorg. Allg. Chem.* **1999**, *625*, 1246–1248.
[29] M. R. Kopp, T. Kräuter, A. Dashti-Mommertz, B. Neumüller, *Organometallics* **1998**, *17*, 4226–4231.
[30] M. L. Durán, J. A. García-Vázquez, C. Gómez, A. Sousa-Pedrares, J. Romero, A. Sousa, *Eur. J. Inorg. Chem.* **2002**, 2348–2354.
[31] K. Kosugi, M. J. Bushiri, N. Nishi, *Appl. Phys. Lett.* **2004**, *84*, 1753–1755.
[32] B. Weber, I. Käpplinger, H. Görls, E.-G. Jäger, *Eur. J. Inorg. Chem.* **2005**, 2794–2811.
[33] M. Weitzer, S. Brooker, *Dalton Trans.* **2005**, 2448–2454.
[34] F. Setifi, S. Golhen, L. Ouahab, A. Miyazaki, K. Okabe, T. Enoki, T. Toita, J. Yamada, *Inorg. Chem.* **2002**, *41*, 3786–3790.
[35] J. Nishijo, A. Miyazaki, T. Enoki, *Bull. Chem. Soc. Jpn.* **2004**, *77*, 715–727.
[36] G. M. Sheldrick, *SHELXS-97*, program for crystal structure determination, and SHELXL-97, program for crystal structure refinement, Institut für Anorganische Chemie der Universität, Tammanstrasse 4, Göttingen, Germany, **1997**.
[37] ORTEP3 for Windows: L. J. Farrugia, *J. Appl. Crystallogr.* **1997**, *30*, 565.

Received: January 24, 2006
Published Online: June 7, 2006

